A compact thermal lithium-beam source using a solid Al/Li alloy for Li sublimation

R. P. Schorn, E. Hintz, S. Musso, and B. Schweer

Institut für Plasmaphysik der Kernforschungsanlage Jülich GmbH, Association EURATOM-KFA, Postfach 1913, D-5170 Jülich, Federal Republic of Germany

(Received 13 April 1989; accepted for publication 22 June 1989)

Thermal lithium beams are widely used in physics for different purposes. To overcome certain disadvantages of conventional liquid-lithium ovens concerning handling, conditioning, and lifetime of the Li filling, a solid Li-evaporation device was constructed. An aluminum-based alloy, which contains about 9 at. % of lithium, is employed. The oven can easily be mounted in any position, and Li atoms can be injected in any desired direction. The parameters of the beam (axial and radial flux profiles) have been measured as a function of temperature and time. At a distance of 100 mm from the oven, Li flux densities of more than 2×10^{14} cm^{-2} s^{-1} have been achieved, lasting for more than 16 days of continued operation. The full beam divergence at half maximum is 8°. As a typical application of the device in plasma diagnostics, radial electron density profiles have been measured in the scrape-off layer of the TEXTOR tokamak.

INTRODUCTION

Thermal lithium beams of the conventional type are employed in many experiments by evaporating pure liquid lithium. Such an oven of the "classic" style has several disadvantages. Liquid lithium is a chemically aggressive substance, especially at elevated temperatures. Cleaning and refilling of the Li reservoir is time consuming and difficult. Elemental lithium being exposed to air is always covered by impurities such as oxides, hydroxides, and compounds of lithium and nitrogen. The first heating of the oven will not only lead to evaporation of lithium, but also to that of the impurities. Furthermore, complications arise, when the beam is to be injected downwards into an experiment. Then, the Li vapor has to be guided by curved ducts, which have to be at a higher temperature than the oven itself. This may lead to a complex experimental setup.

These difficulties can be overcome by applying a solid Al/Li alloy. When the Li concentration is less than 10 at. %, this material remains in the solid state for temperatures below 620 °C, while the lithium component is sublimated. Based on this behavior, a compact thermal lithium-beam source using Al/Li has been constructed. Its design and beam properties, as well as some basic results obtained with it in plasma diagnostics, shall be presented in the following sections.

I. CHARACTERISTICS OF THE LITHIUM ATOMIC BEAM OVEN

As already pointed out in a previous publication,[1] the volatile lithium component of an aluminum-based solid alloy, containing a small amount of lithium, starts to evaporate, when the temperature is raised above 300 °C. According to the phase diagram of the Al/Li system[2] (see Fig. 1), a liquid phase does not exist for temperatures below 620 °C and lithium concentrations below 10 at. %. In this regime, the alloy forms an α phase at elevated temperatures based on the solid-aluminum fcc structure, and a mixed phase consisting of the α phase and the intermetallic compound AlLi (the β phase), which is based on the NaTl-type structure. In both phases, the diffusion coefficient of Li in Al is high enough (5×10^{-9} cm^2/s at 540 °C[3,4]) to compensate evaporation losses by bulk diffusion. According to Ref. 4, the value is nearly independent of the Li concentration. These properties open a possibility to create a thermal lithium atom beam without using the hard-to-handle and chemically aggressive liquid lithium.

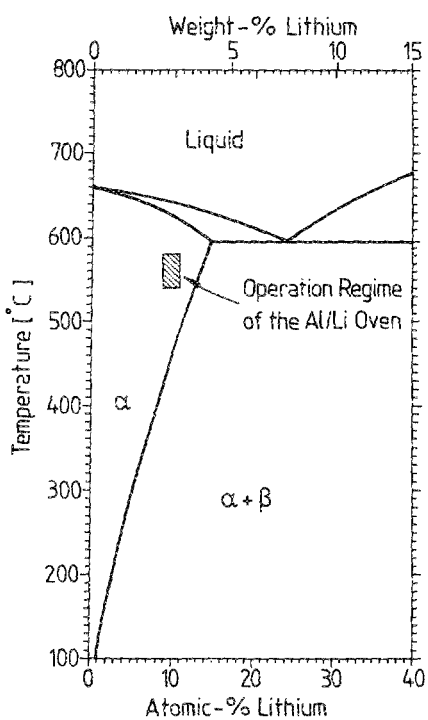

FIG. 1. Part of the phase diagram of the Al/Li system as a redraw from Ref. 2. The Al/Li material is operated in the solid α phase at temperatures close below 600 °C.

 0034-6748/89/103275-05$01.30

In Ref. 1 we have presented flux densities of evaporated monatomic neutral lithium measured by means of laser-induced fluorescence spectroscopy (LIF), calibrated by Rayleigh scattering in argon gas. As another independent absolute calibration method, covering also evaporated ions and Li_2, a quartz oscillator microbalance was used. The principle of the method is described, e.g., in Ref. 5. In order to compare results with those obtained in previous measurements [1], a similar evaporation geometry was used: A plane Al/Li disk (90 mm in diameter, 2 mm thickness) was heated electrically. The surface temperature was monitored by a thermocouple and kept at constant level by an automatic heating system. The quartz plate (of circular shape and 6 mm in diameter) was mounted at a distance of $z = 100$ mm from the emitting disk on the center axis (z axis). The frequency detuning of the quartz oscillator was used to calculate the lithium flux density hitting the quartz surface.

The quartz plate is exposed to lithium evaporation from an extended area. The concept of a point source is not valid here. In order to derive the evaporation rate $\Phi(0)$ at the disk surface from the measured value $\Phi(z)$ at the distance z, the Li emission has to be integrated over the evaporating surface. Provided that the angular emission profile of each surface element is proportional to the cosine of the emission angle, one obtains, for the flux density along the center axis,[6]

$$\Phi(z) = \Phi(0)[1 - z^2/(R^2 + z^2)], \qquad (1)$$

where R is the radius of the disk, and z is the distance from the surface to the position of flux measurement on the axis. In our case, flux densities at $z = 100$ mm have to be multiplied by a factor of 5.9 to get the surface values. Figure 2 shows lithium evaporation rates obtained by this way for temperatures between 400 and 580 °C in an Arrhenius plot. LIF results from Ref. 1 are also shown.

The two curves differ by about 40%, where the LIF technique yields the lower values. To explain this, several reasons have to be considered: The major part of the absolute error is due to the Rayleigh scattering calibration method of LIF. Uncertainties in determining the laser power density (i.e. laser energy, cross section of the beam, and pulse duration) as well as statistical errors of the scattered radiation add up to an error bar of the Li flux of about $\pm$ 40%. The error associated with the quartz balance technique (i.e., determinaton of resonance frequency decay, accuracy of the quartz' material constants) can be estimated to be less than $\pm$ 10%. As Li surfaces easily react with oxygen, nitrogen, and water vapor being contained in the residual gas (here 10^{-7} mbar total pressure), fluxes recorded with a quartz balance may also include certain amounts of adsorbed gases. In our case, however, it can be shown that this amount of "additional flux" is less than 10^{14} cm^{-2} s^{-1} and can be neglected. The content of Li^+ and Li_2 in the beam could not be monitored, but is expected to be less than 10%. Both techniques yield absolute flux values, which agree within the limits of the error bars (see Fig. 2). Moreover, they both reveal about 1.5 eV as energy of vaporization, being typical for elemental lithium. As already concluded in Ref. 1, the alloy surface is predominantly covered by a complete lithium

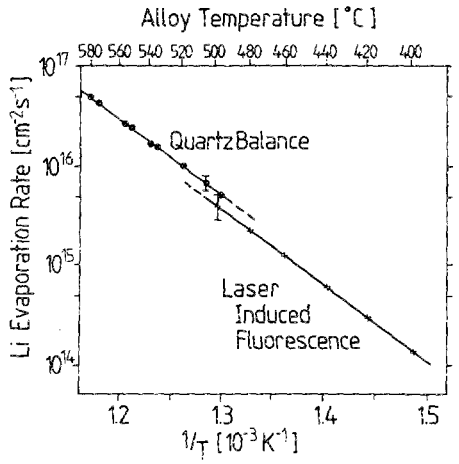

FIG. 2. Temperature-dependent evaporation rates of lithium emitted out of a solid Al/Li alloy. Li fluxes have been measured with laser-induced fluorescence spectroscopy and a quartz microbalance.

overlayer as a result of combined segregation and diffusion processes.

The experimentally determined Li evaporation rates presented above encouraged us to use a closed cavity oven geometry. Lithium then sublimates from an inner surface, and in contrast to the plane disk emitting a broad (cosine) beam into vacuum, a collimation can be achieved. In this way, also the lifetime of the alloy material should be increased. The oven is of a compact cylindrical shape. It is made of a stainless-steel housing heated by a thermocoax and an exchangeable Al/Li alloy insert containing about 9 at. % of lithium. The material, which is applied in aerospace industry, is available from several aluminum producing companies. We have used Al/Li manufactured by Ref. 7. The temperature is measured close to the inner alloy surface by means of a thermocouple. Lithium effuses through a cylindrical collimation duct, which in our case has a diameter of $d = 5$ mm and a length of $l = 15$ mm. A schematic setup of the oven device is shown in Fig. 3.

Again, Li flux densities Φ were measured with a quartz oscillator microbalance at a distance of $z = 100$ mm. The first point of interest was the temporal behavior of Φ. We continuously operated the oven with an alloy mass containing 1.2 g of lithium for more than 16 days at a constant temperature of 540 °C. Figure 4 shows the result. After a steep decrease during the first 2 days, a slowly decreasing flux value of around 1×10^{14}–1.5×10^{14} cm^{-2} s^{-1} is reached. Elevated flux values at the start of operation may be attributed to evaporation of impurities of higher atomic mass, such as lithium oxides, lithium hydroxides, and compounds of lithium and nitrogen, which initially are present on the alloy surface before the first heating. The almost exponential decay of recorded fluxes during the first few days gives rise to this assumption. Using the full spatial beam divergence of $\theta = 8°$ at half maximum (see below), the total evaporated lithium mass can be calculated by integrating the curve in Fig. 4 with respect to time and area. In our case 3×10^{20} atoms, which is less than 0.5% of the alloy insert's total lithium content, have been emitted through the effusion duct during the 16 days of operation. Thus, we are en-

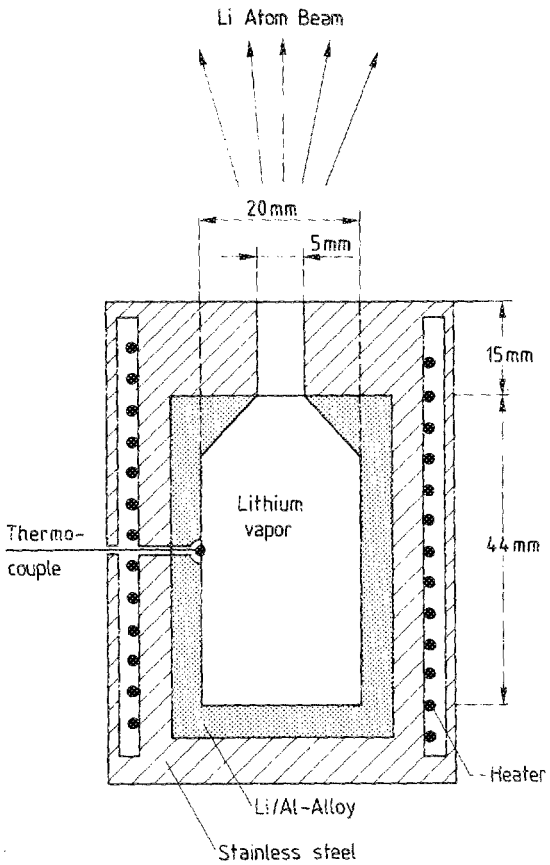

FIG. 3. Setup of the Al/Li oven: An exchangeable alloy insert is heated electrically with a thermocoax. The temperature is measured close to the inner insert surface. The effusion duct used here was 5 mm in diameter and 15 mm in length.

couraged to estimate the effective operation period (i.e. the lifetime) of one insert to be of the order of several months. Interrupting the evaporation process by lowering the temperature, e.g., at weekends, have no effect on the evaporation rate after restarting.

Next, we have investigated the temperature dependence of the lithium emission by the solid oven using the quartz

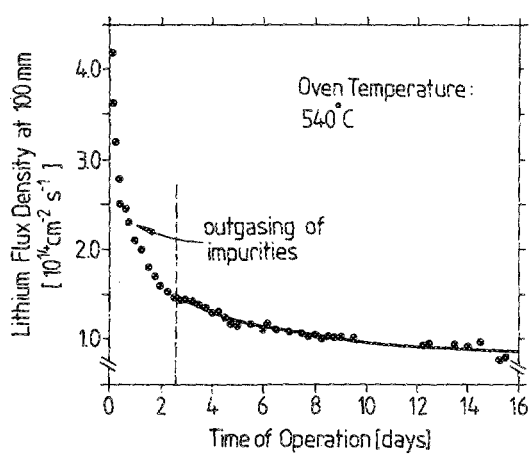

FIG. 4. Longtime performance of the lithium sublimation at 540 °C. The steep decrease during the first 2 days is attributed to evaporation of impurities such as oxides and other compounds of lithium.

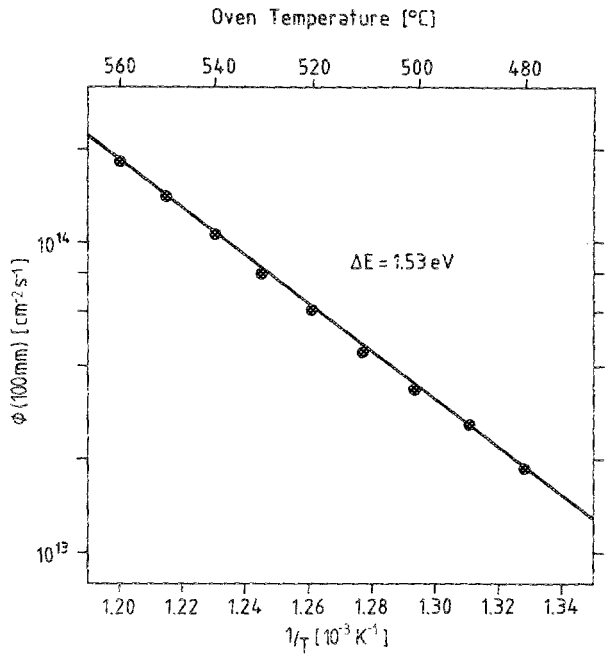

FIG. 5. Temperature dependence of the lithium emission of the oven. The energy of vaporization is determined to be 1.53 eV. Fluxes have been measured with a quartz microbalance at $z = 100$ mm.

balance. Figure 5 shows Li flux densities in the temperature range of 480–560 °C measured at a normal distance of 100 mm. As expected, they follow the well-known Arrhenius relation

$$\Phi(T) = \Phi_0 \exp(-\Delta E/kT), \tag{2}$$

where T is the absolute temperature of the inner alloy surface. We derive an energy of vaporization of $\Delta E = 1.53$ eV, which is in good agreement with the standard value for elemental lithium (1.54 eV[8]). The lithium layer deposited on the quartz balance's surface was analyzed by means of PIXE (proton induced x-ray emission), in order to ensure that the beam did not contain other elements beyond an acceptable percentage. These measurements were kindly performed by the Max-Planck-Institut für Plasmaphysik in Garching.[9] After the above mentioned "conditioning time" of roughly 2 days, when probably also impurities are evaporated, we found that the aluminum particle content in the beam was less than 10^{-6} and the atomic concentration of other impurities (Zn, Ar, S, and Mg) was less than 10^{-4} in total. A coverage of the quartz plate by oxygen, hydrogen, and nitrogen could not be monitored with PIXE. The quartz' surface analysis with PIXE and the outgassing behavior of the Al/Li material lead us to the conclusion that the thermal beam predominantly consists of lithium after the above-mentioned conditioning time.

In Fig. 6 the spatial decay of $\Phi(z)$ along the center axis is depicted. Flux density values are normalized to the $z = 100$ mm position. The knowledge of this curve is important for application of the beam in plasma diagnosites, e.g., when absolute electron densities have to be calculated from recorded lithium photon emission profiles (for details see Sec. II). In the examined distance of 40–140 mm from the effusion duct, fluxes vary by a factor of roughly 7. To obtain

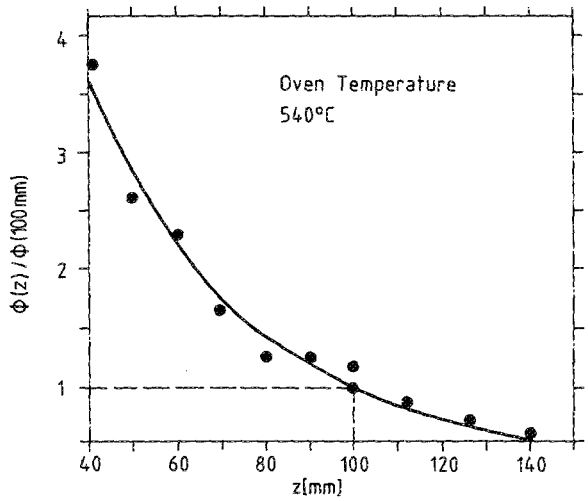

FIG. 6. Spatial decay of the lithium flux density along the center axis

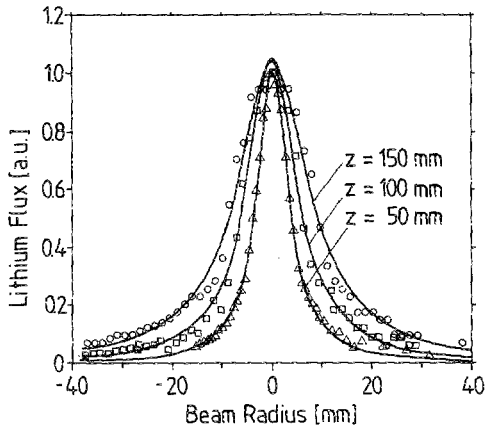

FIG. 7. Radial profiles of the lithium beam at three different distances from the effusion duct. The profiles are normalized to unity. The beam's full divergence at half maximum is calculated to be 8°. Fluxes have been measured with a Langmuir–Taylor detector.

the solid curve in Fig. 6, Eq. (1) was generalized using a $\cos^n$-emission profile and fitted to the data points. This profile has been obtained again with the quartz balance. The oven was mounted on a manipulator, which could be moved in the z direction.

The radial dimensions of the lithium beam have also to be known. As the quartz balance does not give sufficient spatial resolution (the quartz disk has a diameter of 6 mm), and the water-cooled supporting system of the oscillator could not be moved radially, a so-called "Langmuir–Taylor detector" was built. Due to their relatively low energy of ionization, lithium atoms are easily ionized when hitting a hot platinum surface: High efficiencies are obtained when a metal is used, the work function of which approaches the energy of ionization of lithium. This is described quantitatively by the Saha–Langmuir equation.[10] We used a platinum wire of 0.5-mm diameter, which was heated electrically to temperatures around 1800 K. The active length being hit by lithium atoms was limited to 1 mm. Ionized Li atoms were extracted by a catcher electrode at 500 V. The measured current is proportional to the lithium flux impinging onto the platinum wire. The Langmuir–Taylor detector was mounted on a radial manipulator system, so that beam profiles could be recorded also in this direction. Figure 7 shows three radial profiles at distances of $z = 50$, 100, and 150 mm, respectively. At 150 mm, which is the outmost distance to be used at the TEXTOR tokamak (see below), the lithium beam has a diameter of 18 mm FWHM. A beam divergence of 8° FWHM can be calculated from the data in Fig. 7. Beam divergences and radial profiles can be altered by changing the dimensions of the effusion duct. A detailed description of the measurements using a Langmuir–Taylor detector can be found in Ref. 11.

It should be noted that the measurements of radial and axial flux profiles are not totally independent of each other. The sensitive quartz surface being exposed to the Li beam has a finite diameter of 6 mm, while the platinum wire of the Langmuir–Taylor detector extends to 1 mm. Expecially at closer distances from the oven's exit duct, integration over the spatial emission profile leads to altered radial and axial profiles as a consequence.

II. APPLICATION TO THE TEXTOR TOKAMAK: MEASURING ELECTRON DENSITY PROFILES

The Al/Li oven described above can be used successfully in plasma diagnostics. Here, one application is the measurement of electron density profiles in the boundary region of tokamaks: The performance of present day nuclear fusion experiments of the tokamak type suffers from plasma-wall contact, leading to plasma contamination by wall atoms. When studying these interactions, the knowledge of n_e profiles is essential for a description of the boundary layer. Diagnostic methods to determine n_e with a high spatial resolution have been developed in the past, using lithium atom beams of different energies (thermal, laser ablated suprathermal, and several keV). They are injected radially into the scrape-off layer plasma. The principle of the method[12–16] and its application to TEXTOR have been described in detail previously.[13–15,17,18] Therefore, only a short outline shall be given: Due to collisions with plasma electrons, a certain fraction of the Li atoms, which initially are in the $2\,^2S_{1/2}$ ground state, will be excited to higher electronic states. The decay from the lowest excited level ($2\,^2P_{1/2,3/2}$ doublet) leads to photon emission at the Li resonance line of 670.8 nm, which can be observed with excellent radial and temporal resolution. Since the ratio of the ionization function $\langle \sigma_I v_e \rangle$ and the excitation function $\langle \sigma_{s\to p} v_e \rangle$ is only weakly depending on the plasma temperature above 10 eV,[19] lithium beams offer excellent possibilities to monitor the temporal evolution of boundary layer n_e profiles in tokamak discharges. The spatial resolution is about 1 mm.

The Al/Li oven described above has been installed at the TEXTOR tokamak. Figure 8 shows the experimental arrangement. In order to achieve the necessary lithium flux density of 2×10^{14} atoms/cm^2 s for a sufficient Li emission signal, the exit hole is moved to the position of the radius of the liner wall, the oven itself being placed on a movable supporting system. The oven temperature is kept constant within 3° at 560 °C. As shown in Sec. I, the FWHM of the beam is 18 mm at a distance of 150 mm. An automatic shutter prevents lithium from entering the torus between shots, as the

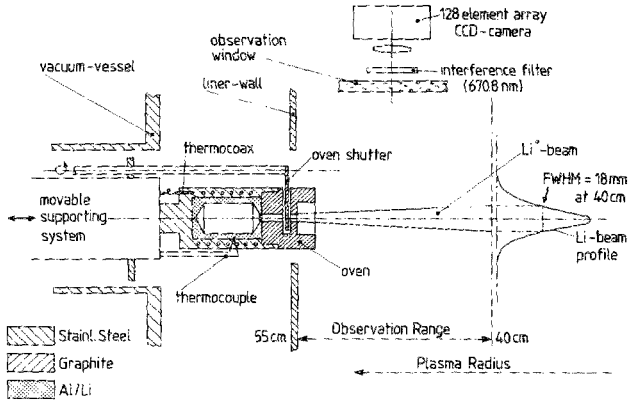

FIG. 8. Experimental setup of the Al/Li oven at TEXTOR: The oven is placed on a movable support unit, the effusion duct being positioned at the liner-wall radius. A shutter prevents Li from entering TEXTOR between discharges. The Li light emission profile is imaged onto a linear array CCD camera.

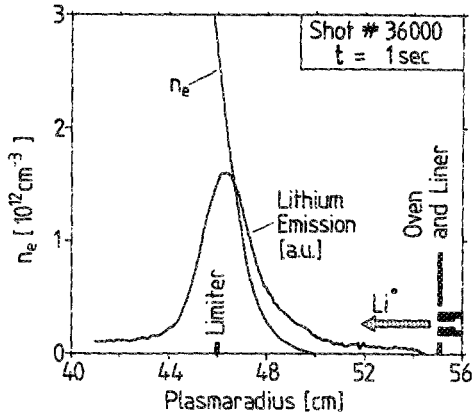

FIG. 9. A typical electron density profile in the scrape-off layer of TEXTOR measured with the Al/Li oven (shot No. 36000). Here, all limiters were positioned at a plasma radius of 46 cm. The profile was recorded 1 s after the start of the tokamak discharge in the flat top phase. The original light emission profile is also plotted.

contamination of the vacuum vessel with Li should be minimized. Radial emission profiles of the Li resonance line are imaged onto a linear array CCD camera, consisting of 128 pixels (Reticon G128/10), the spatial resolution being 1.2 mm in radial and 12 mm in toroidal direction. These profiles can be recorded with a maximum repetition frequency of 2 kHz.

Unwanted radiation, originating from atoms or molecules other than Li, has to be blocked by a narrow interference filter at 670.8 nm. Background radiation from singly ionized oxygen atoms at 672.1 nm seems to be dominating. Therefore, the spectral width of the filter should not exceed 5 Å. The oven surface surrounding the exit duct is exposed to the boundary plasma during shots. In order to reduce the oxygen density in the observation volume, the stainless-steel cap of the oven has been replaced with graphite. A typical electron density profile (TEXTOR shot No. 36000) measured with the setup described above is shown in Fig. 9. This discharge was heated only by the plasma current; no additional heating method was applied. The data curve was taken during the flat top phase at $t = 1$ s, while the total shot duration was 3 s. All limiters were positioned at a plasma radius of 46 cm. The n_e profile was derived from the emission profile by the algorhythm published in Ref 17. Because the lithium-beam density decreases considerably in the observation volume (see data in Sec. I), the emission profile has to be convoluted with the flux decay curve of Fig. 6. The radial beam profiles (Fig. 7) have also to be taken into consideration, as the toroidal extension of the camera array's image amounts to 12 mm in the observation plane. Up to now, we have achieved for a single Al/Li insert more than 100 days of TEXTOR operation. Lithium fluxes decreased only very little during this time. The system is operated on an automatic basis, i.e., heating up in the morning and cooling down in the evening as well as starting the digital data-acquisition system is initiated by automatic devices.

In conclusion, we state that an easy to handle, compact thermal lithium-beam source has been developed and tested at TEXTOR, where electron density profiles have been obtained in the edge plasma region. Long operation periods of more than 100 days have been achieved, without the necessity of breaking the vacuum for maintenance and for refilling of Al/Li material. As a future application, we intend to install at least one additional oven situated at a different poloidal position at TEXTOR.

[1] R. P. Schorn, H. L. Bay, E. Hintz, and B. Schweer, Appl. Phys. A **43**, 147 (1987).
[2] A. J. McAlister, Bull. Alloy Phase Diagr. **3**, 177 (1982).
[3] L. P. Costas, USAEC-Report TID-16676 (1963).
[4] C. J. Wen, Ph.D Dissertation, Stanford University, 1980.
[5] G. Sauerbrey, Z. Phys. **155**, 206 (1959).
[6] E. Dullni, Ph.D. dissertation, University of Bochum, and KFA-Report Jül-1936, July 1984.
[7] Al/Li 80/90F, Pechiney Corporation, Graf-Adolf-Strasse 41, D-4000 Düsseldorf, West Germany.
[8] F. Kohlrausch, *Praktische Physik* (Teubner, Stuttgart, 1986), Vol.3, pp. 259–260.
[9] J. Roth and W. M. Wang (private communication).
[10] S. Datz and E. H. Taylor, J. Chem. Phys. **25**, 389 (1956).
[11] R. Bisenius, engineering diploma thesis, Fachhochschule Aachen, Abteilung Jülich, October 1987.
[12] K. Kadota, K. Matsunaga, H. Igushi, M. Fujiwara, K. Tsuchida, and J. Fujita, Jpn. J. Appl. Phys. **21**, L260 (1982).
[13] P. Bogen, H. Hartwig, E. Hintz, K. Höthker, Y. T. Lie, A. Pospieszczyk, U. Samm, and W. Bieger, J. Nucl. Mater. **128 and 129**, 157 (1984).
[14] Y. T. Lie, K. Höthker, W. Bieger, and K. Kadota, in *Proceedings of the International Conference on Plasma Physics*, Lausanne, Switzerland, 1984.
[15] P. Bogen and E. Hintz, in *Physics of Plasma-Wall Interactions in Controlled Fusion*, edited by D. E. Post and R. Behrisch (Plenum, New York, 1986), p. 211.
[16] K. McCormick and the ASDEX-Team, Rev. Sci. Instrum. **56**, 1063 (1985).
[17] A. Pospieszczyk and G. G. Ross, Rev. Sci. Instrum. **59**, 605 (1988).
[18] A. Pospieszczyk, F. Aumayr, H. L. Bay, E. Hintz, P. Leismann, Y. T. Lie, G. G. Ross, D. Rusbüldt, R. P. Schorn, B. Schweer, and H. Winter, J. Nucl. Mater. **574**, 162 (1989).
[19] N. Brenning, J. Quant. Spectrosc. Radiat. Transfer **24**, 298 (1980).